Scilight

Food Science and Processing

https://www.sciltp.com/journals/fsp

Article

Check for updates

Heterogeneous Australian Pigeonpea [*Cajanus cajan* (L.) Millsp.] Genotypes with Homogeneous *in-vitro* Proteolysis

Danica Malau and Peter A. Sopade *

Food Process Engineering Consultants, Abeokuta Cottage, Tia Lane, Forest Lake, QLD 4078, Australia
* Correspondence: pade_sopade@hotmail.com or peter.sopade@qq.com

How To Cite: Malau, D.; Sopade, P.A. Heterogeneous Australian Pigeonpea [*Cajanus cajan* (L.) Millsp.] Genotypes with Homogeneous *in-vitro* Proteolysis. *Food Science and Processing* **2026**, *2*(2), 8. https://doi.org/10.53941/fsp.2026.100008

Received: 21 February 2026
Revised: 9 May 2026
Accepted: 12 May 2026
Published: 22 May 2026

Abstract: Pigeonpea is a potential raw material for the growing plant protein industry, and the food properties of six Australian genotypes (ICPLs 14425, 86022, 88039, 90048, 91039, and 98011) were investigated. *In-vitro* proteolysis was analysed with a pH drop. The genotypes, coloured cream to brown, differed ($p \leq 0.05$) in their total (43.3–56.5), whiteness (40.2–53.4), yellowish (35.4–50.7), and browning (32.1–60.2) colour indices. Potassium, phosphorus, and sulphur were the major minerals. Approximating a sphere (mm, major [6.6] and minor [6.0] diameters, and thickness [5.3]), the genotypes differed in starch (20–32 g/100g solids) and protein (22–27 g/100g solids) contents. Although the genotypes revealed identical pasting ($p > 0.05$) temperatures (85 ± 2 °C) and slightly-shear thinning behaviours (breakdown ratio = 0.8–0.9), their peak (124–371), trough (108–337), and final (213–520) viscosities (cP) differed. Essentially, the genotypes were heterogeneous in their physicochemical, colour, and pasting properties. However, their protein digestograms, analysed with the Sopade Objective Procedure (objective logarithm of slope), revealed a true monophasic digestion mode; homogeneous *in-vitro* proteolysis. Seven kinetic models for monophasic digestograms adequately ($r^2 > 0.78$) described the digestograms, and the Peleg model was recommended. There were no genotypic differences ($p > 0.05$) in the protein hydrolysis index ($HI_{PROTEIN}$ = 17.4–24.7%) relative to reference casein, average *in-vitro* protein digestibility ($IVPD_{AVG}$ = 69–71%), rate of protein digestion (K_{PR} = 0.09–0.24 min^{-1}), and other protein digestion parameters. This study pioneers time-course protein digestion for pigeonpea, and with rates of food digestion valuable in future food labelling, a solid foundation for pigeonpea utilizations is presented.

Keywords: rate of protein digestion; protein hydrolysis index; *in-vitro* protein digestibility; Sopade Objective Procedure (objective logarithm of slope); monophasic protein digestograms; pH drop

1. Introduction

Pigeonpea [*Cajanus cajan* (L.) Millsp.] is the world's sixth most important edible legume or pulse and a warm-season, drought-tolerant, and nitrogen-fixing perennial crop that grows in tropical and subtropical regions [1–5]. Pigeonpea is mainly grown in Africa, the Caribbean, and South Asia, and its global production increased by about 50% from 2003 to 2023; 4.6 million MT, 2023; 3.1 million MT, 2003 [6]. India, Malawi, Myanmar, Tanzania, the Dominican Republic, and Haiti are among the top 10 pigeonpea-producing countries [6]. Pigeonpea is also referred to as adhaki, Congo pea, dhal, no-eye pea, Pois d'Angole, Puerto Rico pea, quinchoncho, red gram, tur, and urhur [5,7,8], among other local names in the producing nations. Many pigeonpea varieties, cultivars, genotypes, or hybrids have been reported with black, brown, cream, dark brown, off-white, purple, and white seed coats [9–13]. Tiwari et al. [13]

reported 20, Kachare et al. [10] studied 25, Yohane et al. [14] examined 80, and Ravika et al. [11] and Sultana et al. [9] respectively investigated 175 and 272 pigeonpea genotypes. Five varieties have recently [15] been released in Australia for improved yield, shorter crop cycle, reduced height, and optimum seed size, among other agronomical attributes, to meet the growing global demand for pigeonpea. Locali-Pereira et al. [3] had earlier itemised the need to breed improved varieties to cement pigeonpea as a major world commodity, more so, for the growing plant protein industry that could be over US$27 billion by 2030 and US$40 billion by 2035 [2,16,17]. However, pigeonpea is largely considered an orphan or underutilised crop or a crop that is yet to be fully utilised or properly explored [4,5,7,18,19]. The increasing demand for pigeonpea is, however, encouraging even in Australia as a summer crop [2,20,21], and the nutraceutical properties of pigeonpea drive this demand.

Pigeonpea is a rich source of dietary protein, carbohydrates, minerals, polyphenols, and some amino acids and vitamins, and it possesses anti-inflammatory, -bacterial, -oxidant, -carcinogenic, -dyslipidemic, and -diabetic properties [4,5,11,19,22,23]. It has been used in traditional medicines to treat various ailments, and both Oluwole et al. [22] and Haji et al. [5], for example, extensively discussed the benefits of pigeonpea in human health and nutrition. However, despite its content of essential amino acids for health and nutrition, the digestibility of pigeonpea proteins is, characteristic of legume or pulse proteins, adversely affected [3,13,16,24,25] by antinutritional factors (e.g., cyanogenic glycosides, hemagglutinin, lectins, oligosaccharides, phytates, polyphenols, protease inhibitors, saponins, and tannins). Apart from food structures and matrices influencing digestibility, these antinutrients reduce digestive enzyme activities, bind proteins to hinder proteolysis, and interfere with digestion to trigger metabolic disorders [26]. Various studies have, therefore, been conducted [25,27–29] to understand and optimise protein digestibility of pigeonpea. These studies mainly used *in-vitro* techniques for their relative advantages over *in-vivo* techniques [3,30–32]. Processed (soaking, heat-moisture, germination, extrusion, etc.) and non-processed pigeonpea samples were investigated [3], with the latter providing foundational understandings of processing effects. These *in-vitro* protein digestibility studies were essentially conducted [13,18,19,23,28,31] as single-point measurements. But single-point measurements of food digestion are relatively limited on digestion mechanisms [32–34] compared to time-course measurements. Unlike single-point measurements, time-course measurements yield protein digestograms that are described by kinetic models to reveal digestion modes (mono- and multi-phasic) and phenomena (rapid-slow, slow-rapid, rapid-slow-slow, etc.). The kinetic parameters are then better quantitatively and objectively analysed for in-depth mechanisms of protein digestion [32,35]. For example, rates of protein digestion, not obtainable from single-point measurements, are an important digestion parameter, and Lao et al. [26] observed that rates of protein digestion define protein roles in food systems for fast and slow nutrient releases and protection. Mackie [30] discussed the benefits of fast digestion and absorption of proteins, which are dependent on rates of protein digestion. Hence, rates of food digestion are becoming or will become a focus, and food labelling of the future might require such to make time-course measurements of food digestion the gold standard. Incidentally, the kinetics of protein digestion in pigeonpea are relatively non-existent, and more importantly and specifically, none on Australian genotypes, cultivars, or varieties to help understand the differences or similarities resulting from homogenous or heterogenous physicochemical and functional properties. The present study, therefore, investigated time-course *in-vitro* protein digestibility of six genotypes of pigeonpea grown in Queensland, Australia and described the resulting digestograms with kinetic models. The hypothesis was that the genotypes are heterogeneous in their food (physicochemical, functional, and protein digestibility) properties.

2. Materials and Methods

2.1. Materials

Six genotypes of pigeonpea (from the International Crop Research Institute for the Semi-Arid Tropics Pigeonpea Line, ICPL) ICPLs 14425, 86022, 88039, 90048, 91039, and 98011, grown in Australia, were obtained from the Queensland Department of Agriculture and Fisheries, Kingaroy, Australia. The grains were manually cleaned, and only sound, whole ones were analysed. Some of the grains were cryomilled (6850 SPEX Freezer/Mill; SPEX, Metuchen, NJ 08840, USA: pre-cooling time, 5 min; cycle, 2; time between cycles, 2 min; grinding time per cycle, 5 min; impactor (stainless steel, diameter ≈ 19 mm, length ≈ 70 mm) speed, 10 s^{-1} [36,37], and both the milled and whole gains were stored (≈ 3 °C) in air-tight containers prior to analyses.

2.2. Physicochemical Properties

2.2.1. Chemical Properties

Ash (muffle furnace, 600 °C, 4 h), crude fat (petroleum spirit, 25 mm diameter × 80 mm height thimbles, Soxhlet method), moisture (oven-dry, 105 °C, 16 h), protein (N × 6.25, LECO combustion analyser, 950 °C, total

N_2), and total starch (Megazyme™ method) contents of the ground samples were measured as before [38,39]. Non-starch polysaccharides were calculated by difference.

2.2.2. Mineral Analysis

Inductively Coupled Plasma with Optical Emission Spectroscopy (ICP-OES) equipment (Vista Pro, Varian Scientific Instruments Pty Ltd., Mulgrave, VIC, Australia) as described in Waramboi et al. [40] was used to measure the minerals in the ground samples.

2.2.3. Physical Properties

Ten sound grains of each genotype were randomly selected, and their major diameter (MA), minor diameter (MI), and thickness (TH) were measured with Vernier Callipers. Twenty of such grains were selected, in five replicates, and weighed to calculate the 1000-grain weight. The geometric mean diameter (GMD) of the genotypes was calculated [41]:

$$\mathrm{GMD} = \sqrt[3]{(\mathrm{MA} \times \mathrm{MI} \times \mathrm{TH})} \quad (1)$$

2.2.4. Colour Properties

The L, a, and b colour values of the ground samples ($_{gen}$) and a reference white tile ($_{ref}$) were measured (Model CR-400, Konica Minolta Sensing Inc., Sakai-ku, Japan) in triplicate, and the total colour (ΔE), Chroma (colour saturation and intensity), Hue angle (0, red; 90, yellow; 180, green; 270, blue; and 360, red), and browning (BI, purity of brown colour), yellowish (YI, purity of yellow colour), and whiteness (WI, purity of white colour) indices were calculated [17,39,42]:

$$\Delta E = \sqrt{(L_{gen} - L_{ref})^2 + (a_{gen} - a_{ref})^2 + (b_{gen} - b_{ref})^2} \quad (2)$$

$$\mathrm{Chroma} = \sqrt{{a_{gen}}^2 + {b_{gen}}^2} \quad (3)$$

$$\text{Hue angle} = \tan^{-1}\left(\frac{b_{gen}}{a_{gen}}\right) \quad (4)$$

$$\mathrm{BI} = \frac{100\,(X - 0.31)}{0.17}$$

$$x = \frac{a_{gen} + 1.75\,L_{gen}}{5.645\,L_{gen} + a_{gen} - 3.012\,b_{gen}} \quad (5)$$

$$\mathrm{WI} = 100 - \sqrt{(100 - L_{gen})^2 + {a_{gen}}^2 + {b_{gen}}^2} \quad (6)$$

$$\mathrm{YI} = \frac{142.86\,b_{gen}}{L_{ge}} \quad (7)$$

2.3. Pasting Properties

The pasting properties of the ground samples (2.5 g solids in 25 g total weight with distilled water; 10% *w*/*w*, solids) were studied with the Rapid Visco-Analyser (RVA-4, Newport Scientific Pty Ltd., Warriewood, NSW, Australia) using the RVA Standard Profile 1 procedure [39,40]. In addition to the traditional pasting viscosities or parameters, the breakdown ratio (BDR) was defined (Trough viscosity/Peak viscosity) and used [40] to classify pasting behaviours as highly-shear thinning (<0.5), moderately-shear thinning (0.5–0.8), slightly-shear thinning (0.8–1.0), or shear thickening (>1.0).

2.4. In-Vitro Protein Digestibility

The pH-drop method of Hsu et al. [43], with modifications [35,44,45], was used. The ground samples (equivalent to 62.5 g dry protein) were rehydrated (10 mL milli-Q, 37 °C, 60 min., pH ≈ 8.0) and treated with 10 mL of a fresh trypsin-chymotrypsin-protease mixture (16:31:13, *w*/*w*; 37 °C; pH ≈ 8.0). The pH of the digesta was

periodically recorded to define cumulative changes in pH (ΔpH_i) from the starting pH and time (t) data for protein digestograms, from which *in-vitro* protein digestibility ($IVPD_{10min.}$) was calculated:

$$IVPD_{10min.} = 65.66 + 18.10\ \Delta pH_{10min.} \quad (8)$$

where $\Delta pH_{10min.}$ = change in pH at 10 min. Casein (Sigma C7078; casein from bovine milk) was the reference, and the analysis was duplicated. Additionally, predicted IVPD (pIVPD from hydrolysis index of protein, $HI_{PROTEIN}$) and average IVPD ($IVPD_{AVG}$) were calculated as before [32,35,45]:

$$pIVPD = 0.29\ HI_{PROTEIN} + 61.89 \quad (9)$$

where $HI_{PROTEIN}$ = (100 × Area Under Digestogram of Sample, AUC_{sample}/Area Under Digestogram of Casein, AUC_{casein}).

$$IVPD_{AVG} = (IVPD_{10min.} + pIVPD)/2 \quad (10)$$

Slope Changes or Discontinuities for *in-Vitro* Protein Digestion Modes

The duplicated digested protein-time data were pooled to plot logarithm of slope, LOS, ($\ln \{[\Delta pH_{i+1} - \Delta pH_i]/[t_{i+1} - t_i]\}$) against time ($t_i$) of LOS, TLOS, ($[t_{i+1} + t_i]/2$) and described by linear (order 1), quadratic (order 2), and cubic (order 3) polynomial equations [32,35,45]. The appropriate first and/or second derivative(s) were/was used to objectively interpolate slope changes/discontinuities (Sopade Objective Procedure, objective logarithm of slope). The slope changes guided the preliminary *in-vitro* protein digestogram classes, phases, or segments of the samples and consequently, digestion modes (mono- and multi-phasic) for appropriate kinetic models to describe the digestograms.

2.5. Statistical Analysis

The ground or whole seeds (grains) of the genotypes were randomly analysed, at least, in duplicate ($n \geq 2$), and Microsoft Excel (Microsoft 365) was used for analysis of variance, χ^2-test, *t*-test, confidence intervals, and linear and nonlinear regressions. In modelling the protein digestograms, the sum of squares of residuals (SUMSQ) was minimised for the nonlinear regression, with constraints ($\Delta pH_{t=0} \geq 0$, $IVPD_{10min} \leq 100$ g/100 g dry protein, $\Delta pH_{t\to\infty} \leq 6.0$) to prevent impractical protein digestion parameters. Coefficient of determination [r^2], mean relative deviation modulus [MRDM], and/or SUMSQ were/was the predictability indices/index for the equations or models investigated [32,35,45].

3. Results and Discussion

3.1. Chemical Properties

Table 1 shows the physicochemical and functional properties of the Australian pigeonpea genotypes, and typical of legumes or pulses, the protein content (g/100 g solids) ranged from about 22–27 g/100 g solids. The ash and fat contents were 1–2 g/100 g solids, while the starch and non-starch polysaccharides (approximately carbohydrates by difference) were at least 50 g/100 g solids. The samples were significantly ($p \leq 0.05$) different in their proximate composition, with values that align with other studies [7,19,23,46]. Bustin et al. [47] and Thomas et al. [29] reported inverse correlations between starch, fat, and protein contents for some pulses and legumes. However, the pigeonpea genotypes revealed non-significant inverse starch-protein and starch-fat trends. The major and minor minerals, significantly ($p \leq 0.05$) and non-significantly ($p > 0.05$) different among the genotypes, are summarised in Supplementary Table S1. Various authors have reported the mineral contents of pigeonpea. For example, Oloyo [48] measured calcium, magnesium, iron, copper, manganese, and phosphorus in one variety and found calcium and phosphorus as the highest minerals, with copper and manganese being the lowest. Sangronis and Machado [49] measured calcium, magnesium, zinc, iron, and copper in another variety and found calcium and magnesium to be the highest, with the lowest minerals being zinc and copper. In a study [19] that measured iron, copper, manganese, and zinc contents of another variety, copper was of the lowest concentration, and iron and zinc were higher. Chinma et al. [23] reported calcium to be about 100× iron and zinc in their pigeonpea sample. The present study (Supplementary Table S1) revealed potassium, phosphorus, sulphur, magnesium, and calcium as the major minerals in the six Australian pigeonpea genotypes, while sodium, copper, manganese, and aluminium were the minor minerals. Relatively, therefore, pigeonpea is a poor source of copper and manganese but a good source of potassium, phosphorus, sulphur, magnesium, and calcium, which consistently are of the highest concentrations. Dutta et al. [28] and Haji et al. [5] reported the latter as the major minerals in pigeonpea, and Locali-Pereira et al. [3] reported pigeonpea as a richer source of calcium than common beans and chickpeas.

Table 1. Physicochemical and functional properties of the Australian pigeonpea genotypes.

Parameter	ICPL 14425	ICPL 86022	ICPL 88039	ICPL 90048	ICPL 91039	ICPL 98011
A. Chemical properties (g/100 g solids)						
Moisture	16.3 ± 0.0 ^{ae}	17.9 ± 0.0 ^{abc}	19.4 ± 1.1 ^{a}	17.7 ± 0.0 ^{ad}	17.3 ± 0.9 ^{bcde}	18.0 ± 0.0 ^{ab}
Fat	1.0 ± 0.0 ^{cd}	1.3 ± 0.1 ^{ac}	1.5 ± 0.1 ^{ab}	1.6 ± 0.1 ^{a}	1.3 ± 0.1 ^{ad}	1.3 ± 0.2 ^{abc}
Ash	1.1 ± 0.0 ^{bcd}	1.1 ± 0.0 ^{bc}	1.2 ± 0.0 ^{a}	1.1 ± 0.0 ^{abcd}	1.1 ± 0.0 ^{d}	1.1 ± 0.0 ^{b}
Protein	23.5 ± 0.2 ^{bc}	22.5 ± 0.2 ^{bd}	21.6 ± 0.3 ^{cd}	26.3 ± 0.0 ^{a}	23.6 ± 0.2 ^{b}	26.6 ± 0.2 ^{a}
Starch	30.5 ± 0.4 ^{abcd}	32.4 ± 1.3 ^{a}	31.8 ± 0.7 ^{ab}	20.7 ± 0.4 ^{f}	30.9 ± 0.2 ^{abc}	29.7 ± 0.3 ^{abce}
Non-starch polysaccharides	27.5 ± 0.1 ^{b}	24.8 ± 1.2 ^{bc}	24.6 ± 0.0 ^{c}	32.5 ± 0.4 ^{a}	25.8 ± 0.4 ^{bc}	23.2 ± 0.7 ^{c}
B. Physical properties						
Major diameter (mm)	6.3 ± 0.3 ^{c}	6.6 ± 0.4 ^{b}	7.3 ± 0.4 ^{a}	7.1 ± 0.4 ^{a}	6.1 ± 0.4 ^{c}	6.5 ± 0.3 ^{b}
Minor diameter (mm)	6.1 ± 0.3 ^{ab}	6.1 ± 0.4 ^{bc}	6.4 ± 0.5 ^{a}	6.2 ± 0.34 ^{ab}	5.9 ± 0.4 ^{c}	5.4 ± 0.4 ^{d}
Thickness (mm)	5.2 ± 0.2 ^{a}	5.2 ± 0.1 ^{a}	5.4 ± 0.2 ^{a}	5.3 ± 0.3 ^{a}	5.3 ± 0.3 ^{a}	5.2 ± 0.1 ^{a}
Geometric mean diameter (mm)	5.8 ± 0.2 ^{c}	5.9 ± 0.2 ^{c}	6.3 ± 0.3 ^{a}	6.2 ± 0.2 ^{b}	5.7 ± 0.3 ^{cd}	5.6 ± 0.2 ^{d}
1000-grain weight (g)	109 ± 3.0 ^{b}	106 ± 1.7 ^{b}	102 ± 3.0 ^{c}	120 ± 4.8 ^{a}	97 ± 1.9 ^{d}	97 ± 4.0 ^{d}
C. Colour properties						
L	55.6 ± 0.2 ^{a}	54.6 ± 1.1 ^{a}	44.0 ± 0.8 ^{b}	42.6 ± 1.0 ^{c}	43.3 ± 0.6 ^{bc}	42.9 ± 0.5 ^{c}
a	3.1 ± 0.2 ^{f}	5.2 ± 0.6 ^{e}	10.2 ± 0.6 ^{b}	9.6 ± 0.3 ^{bc}	8.4 ± 0.5 ^{d}	11.5 ± 0.4 ^{a}
b	13.8 ± 0.5 ^{bc}	14.6 ± 0.5 ^{ab}	15.6 ± 0.3 ^{a}	13.4 ± 0.8 ^{bc}	13.7 ± 0.3 ^{c}	13.6 ± 1.1 ^{bc}
Hue angle (^{0})	77.3 ± 0.9 ^{a}	70.6 ± 2.2 ^{b}	56.7 ± 1.2 ^{c}	54.3 ± 1.2 ^{e}	58.6 ± 1.0 ^{c}	49.7 ± 2.8 ^{f}
Chroma	14.1 ± 0.5 ^{e}	15.5 ± 0.6 ^{ce}	18.7 ± 0.6 ^{a}	16.5 ± 0.8 ^{bc}	16.0 ± 0.5 ^{bcd}	17.8 ± 0.8 ^{ab}
Whiteness index	53.4 ± 0.1 ^{a}	52.0 ± 1.2 ^{a}	41.0 ± 1.0 ^{bc}	40.3 ± 0.8 ^{b}	41.1 ± 0.7 ^{b}	40.2 ± 0.5 ^{b}
Browning index	32.1 ± 0.9 ^{c}	37.7 ± 2.4 ^{b}	60.2 ± 3.4 ^{a}	53.7 ± 1.8 ^{a}	51.5 ± 2.3 ^{a}	57.1 ± 3.8 ^{a}
Yellowish index	35.4 ± 1.1 ^{e}	38.3 ± 2.0 ^{be}	50.7 ± 2.0 ^{a}	44.9 ± 1.8 ^{abcd}	45.1 ± 1.4 ^{bc}	45.3 ± 3.7 ^{ab}
ΔE (Total colour)	43.3 ± 0.1 ^{d}	44.7 ± 1.2 ^{d}	55.8 ± 1.0 ^{b}	56.5 ± 0.8 ^{a}	55.7 ± 0.7 ^{abc}	56.6 ± 0.5 ^{a}
D. Pasting properties						
Pasting temperature (°C)	84.1 ± 2.3 ^{a}	82.8 ± 3.0 ^{a}	85.0 ± 0.6 ^{a}	86.4 ± 0.4 ^{a}	84.6 ± 1.0 ^{a}	85.5 ± 0.4 ^{a}
Initial viscosity (cP)	25.2 ± 2.0 ^{a}	22.2 ± 4.0 ^{a}	28.1 ± 1.9 ^{a}	30.5 ± 0.1 ^{a}	28.5 ± 2.9 ^{a}	33.1 ± 3.5 ^{a}
Peak viscosity (cP)	200.5 ± 9.2 ^{bc}	209.5 ± 3.5 ^{b}	371.0 ± 2.8 ^{a}	136.0 ± 4.2 ^{d}	137.5 ± 7.8 ^{cd}	123.5 ± 2.1 ^{d}
Trough viscosity (cP)	159.5 ± 3.5 ^{c}	179.5 ± 0.7 ^{b}	336.5 ± 7.8 ^{a}	117.5 ± 4.9 ^{d}	120.0 ± 5.7 ^{d}	108.5 ± 0.7 ^{d}
Breakdown viscosity (cP)	41.0 ± 12.7 ^{a}	30.0 ± 2.8 ^{abc}	34.5 ± 4.9 ^{ab}	18.5 ± 0.7 ^{abc}	17.5 ± 2.1 ^{ab}	15.0 ± 2.8 ^{ac}
Breakdown ratio (BDR)	0.8 ± 0.1 ^{a}	0.9 ± 0.0 ^{a}	0.9 ± 0.0 ^{a}	0.9 ± 0.0 ^{a}	0.9 ± 0.0 ^{a}	0.9 ± 0.0 ^{a}
Final viscosity (cP)	293.0 ± 7.1 ^{bc}	304.5 ± 3.5 ^{b}	519.5 ± 20.5 ^{a}	225.5 ± 0.7 ^{de}	246.0 ± 8.5 ^{cd}	213.0 ± 0.0 ^{d}
Setback viscosity (cP)	133.5 ± 10.6 ^{ab}	125.0 ± 4.2 ^{abc}	183.0 ± 28.3 ^{a}	108.0 ± 5.7 ^{acd}	126.0 ± 2.8 ^{abc}	104.5 ± 0.7 ^{abd}

Non-starch polysaccharides were obtained by difference from 100 g/100 g solids. Values are means ± standard deviations (n ≥ 2). Values in a row with the same letters are non-significant ($p > 0.05$). These apply wherever they appear.

3.2. Dimensional Properties

The dimensions of the pigeonpea genotypes were significantly ($p \leq 0.05$) different but around 6 mm; major diameter (mm) = 6.6 ± 0.5, minor diameter (mm) = 6.0 ± 0.5, thickness (mm) = 5.3 ± 0.2, and geometric mean diameter (mm) = 5.9 ± 0.3 (Table 1). Theoretically, therefore, a spherical shape of diameter 6 mm can be assumed for the genotypes in computations that need a regular shape for certain design characteristics of and for the genotypes. The 1000-grain weight significantly ranged from 97–106 g (Table 1) and is within the range in Singh et al. [50]. Bustin et al. [47] reported inverse and direct correlations between protein content and seed size. However, using the geometric mean diameter and 1000-grain weight as measures of the seed size or weight, the genotypes respectively revealed inverse and direct trends, non-significant ($p > 0.05$) though, with their protein content.

3.3. Colour Properties

The genotypes were heterogeneous in their seed coat colours (Supplementary Figure S1), and the various colour parameters of the ground samples (Table 1) quantify this. The genotypes ICPLs 14425 and 86022, with cream seed coats, were significantly the highest in the L, hue angle, and whiteness index but the lowest in the browning and yellowish indices. The genotypes ICPLs 88039 and 98011, with brown seed coats, significantly had the highest browning and yellowish indices but the lowest whiteness index. The yellowish index of the genotypes significantly ($p \leq 0.05$) correlated with the browning (direct) and whiteness (inverse) indices. Although Kachare et al. [10] and Sultana et al. [9] did not report any colour indices, they studied pigeonpea samples with black, brown, cream, dark-brown, off-white, purple, white, medium-brown, light-brown, and light-grey seed coats. In their study of pigeonpea with light-brown, red-brown, and black seed coat colours, Fasoyiro et al. [1] concluded that seed coat colours influenced sensory acceptability. Plant seed coats or hulls are made up of components of nutritional significance that influence food properties, and the diverse colours of the pigeonpea genotypes point to possible differences in these properties.

3.4. Pasting Properties

The pigeonpea genotypes pasted at about the same temperature (85 ± 2 °C) and to about the same initial pasting viscosity (28 ± 4 cP), as summarised in Table 1, while also exhibiting an identical pasting pattern (Figure 1). The breakdown ratio (BDR), non-significant ($p > 0.5$), averaged 0.87 ± 0.03 to indicate the genotypes were slightly shear-thinning and might present identical structural resistance to shear-induced treatments and processes. Because of pronounced component-component interactions (e.g., starch-protein, starch-lipid, etc.) in plant systems, shear sensitivities vary, and shear-thinning or shear-thickening behaviours can manifest to different degrees [8,44]. Chinma et al. [23] measured a slightly shear-thinning behaviour (BDR = 0.96) in a pigeonpea flour, so did Kumari and Sit [8] in pigeonpea flour (BDR = 1.00) and starch (BDR = 0.89), which the latter authors associated with amylose-amylose, amylose-amylopectin, and amylose-lipid interactions. With more studies, the shear-sensitivity or shear-stability of pigeonpea can be better established, as this influences processing (e.g., extrusion) where shear sensitivities and flow behaviours of raw materials are important for product quality. Wu et al. [4] discussed the benefits of the relatively high pasting viscosity of pigeonpea for food uses. However, despite an identical pasting pattern, the pigeonpea genotypes revealed significant differences in pasting, exemplified in their peak, trough, and final viscosities (Table 1 and Figure 1). With differences in the three macronutrients, fat, protein, and starch (Table 1), which influence pasting, the heterogeneous pasting properties of the genotypes are not unexpected.

3.5. Protein Digestibility

Figure 2 shows the application of the Sopade Objective Procedure, objective logarithm of slope, to the protein digestograms of the samples. The polynomial equations of orders 1–3 suggested apparent biphasic (ICPLs 14425, 86022, 88039, and 90048) and triphasic (ICPLs 91039 and 98011) digestograms for possible heterogeneous *in-vitro* proteolysis of the pigeonpea. No samples, however, preliminarily revealed a monophasic digestion mode. Digestion modes in food systems can be mono-, bi-, or tri-phasic due to component-component interactions or none. Monophasic digestion modes occur in the absence of impediments, while multiphasic modes occur due to impediments, the form of which can lead to two or three phases in food digestograms. Mihalyi and co-workers [51,52] associated multiphasic protein digestion with hydrolytic differences in the number or nature of peptide bonds that result from primary, secondary, and tertiary structures of proteins [32]. However, the preliminary or apparent digestion modes from the polynomial equations need to be critically and statistically examined for the true digestion modes to be deduced or recommended for the samples. With food digestion modes and rates of food digestion potentially valuable in future product developments and labelling expectations, true digestion modes and

associated digestion parameters need to be thoroughly established for heterogeneous or homogeneous *in-vitro* proteolysis in the pigeonpea genotypes and generally food systems. The criterion for true digestion modes or digestogram classes is for rates of digestion to be significantly different or not within 95% confidence intervals of each other, among other heterogeneity tests described elsewhere [32,35,45,53].

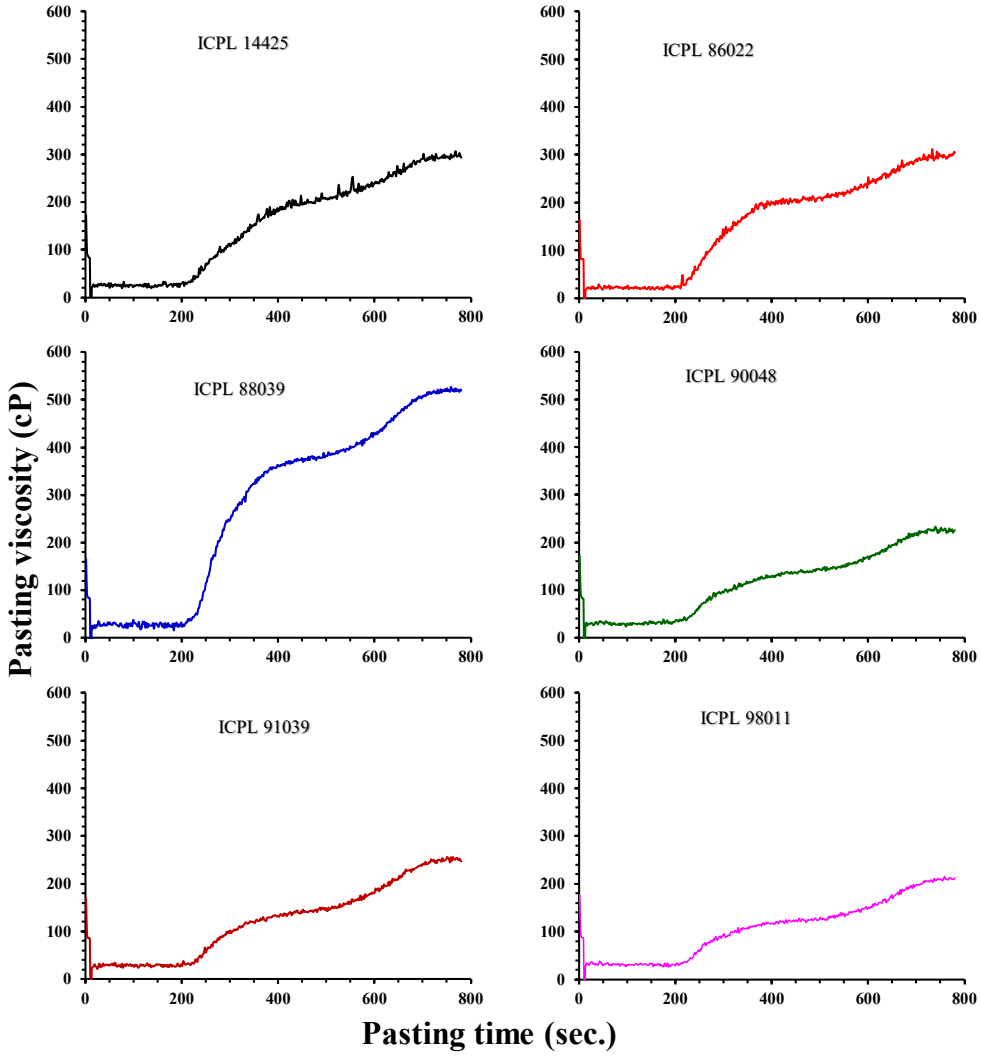

Figure 1. The RVA viscoamylograms of the pigeonpea genotypes. (The temperature profile, not shown, is the RVA Standard Profile 1. Error bars are not shown for clarity, but the coefficient of variation of duplicate analyses per variety averaged 6% [n = 2400]).

For the suggested multiphasic digestion modes in the genotypes, the following multiphasic kinetic models [32,35,43,53,54] were applied to the protein digestograms (ΔpH_t − t data), using non-linear regressions (Microsoft Excel Solver®; minimising SUMSQ; constraints $\Delta pH_0 \geq 0$, $IVPD_{10min} \leq 100$ g/100 g dry protein, $\Delta pH_\infty \leq 6.0$) as discussed above:

3.5.1. Segmented Modified First-Order Kinetic Model

$$\Delta pH_{ti} = \Delta pH_{0i} + \Delta pH_{(\infty\,0)i}\,(1 - \exp\,[K_{Pri}\,t])$$

or

$$\Delta pH_{ti} = \Delta pH_{0i} + (\Delta pH_{\infty i} - \Delta pH_{0i})\,(1 - \exp[\,K_{PRi}\,t]) \quad (11)$$

ΔpH_{ti} = change in pH in phase i at time t, ΔpH_{0i} = change in pH in phase i at an effective t = 0, $\Delta pH_{(\infty\text{-}0)i} = (\Delta pH_{\infty i} - \Delta pH_{0i})$, with $\Delta pH_{\infty i}$ being the change in pH in phase i at time $t \rightarrow \infty$, and K_{PRi} = rate of protein digestion in phase i. Equation (11) is a general equation and applies to both biphasic (i = 2) and triphasic (i = 3) digestion modes, and when i = 1 (see below), it defines a monophasic digestogram.

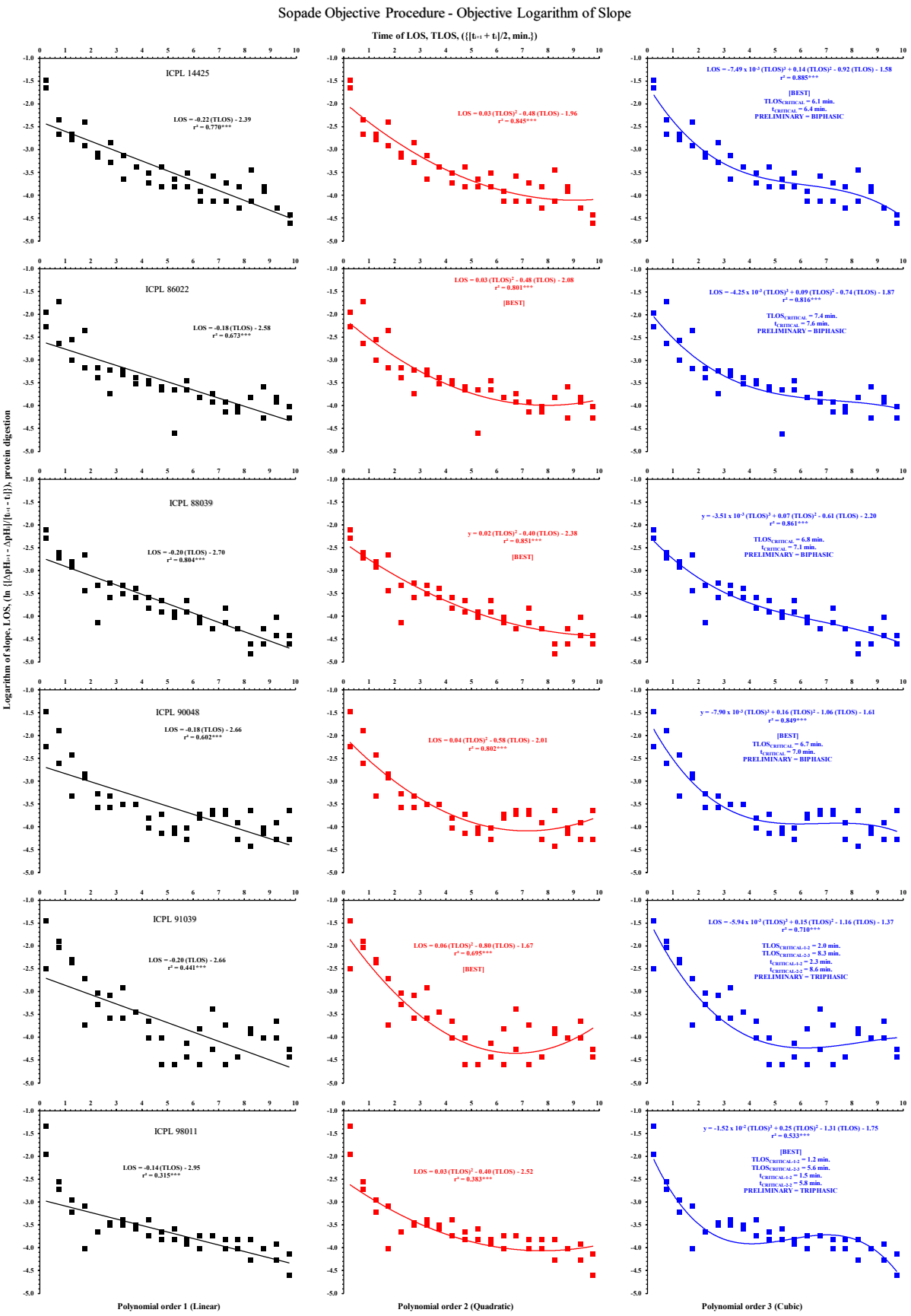

Figure 2. The Sopade Objective Procedure, objective logarithm of slope, with the polynomial equations for the pigeonpea genotypes (*** = $p \leq 0.001$).

3.5.2. Multi-Term Exponential Models

Two-term exponential model for biphasic digestion:

$$\Delta pH_t = \Delta pH_0 + \Delta pH_1 [1 - \exp(-K_{PR1} t)] + \Delta pH_2 [1 - \exp(-K_{PR2} t)]$$

or

$$\Delta pH_t = \Delta pH_\infty - \Delta pH_1 \exp(-K_{PR1} t) - \Delta pH_2 \exp(-K_{PR2} t)$$

$$\Delta pH_\infty = \Delta pH_0 + \Delta pH_1 + \Delta pH_2 \quad (12)$$

Three-term exponential model for triphasic digestion:

$$\Delta pH_t = \Delta pH_0 + \Delta pH_1 [1 - \exp(-K_{PR1} t)] + \Delta pH_2 [1 - \exp(-K_{PR2} t)] + \Delta pH_3 [1 - \exp(-K_{PR3} t)]$$

or

$$\Delta pH_t = \Delta pH_\infty - \Delta pH_1 \exp(-K_{PR1} t) - \Delta pH_2 \exp(-K_{PR2} t) - \Delta pH_3 \exp(-K_{PR3} t)$$

$$\Delta pH_\infty = \Delta pH_0 + \Delta pH_1 + \Delta pH_2 + \Delta pH_3 \quad (13)$$

where ΔpH_t, ΔpH_0, ΔpH_∞, ΔpH_1, ΔpH_2, and ΔpH_3 are respectively changes in pH (ΔpH) at times t, t = 0, and t → ∞, and in phases 1, 2, and 3, while K_{PR1}, K_{PR2}, and K_{PR3} are respectively the rates of protein digestion in phases 1, 2, and 3.

3.5.3. Multi-Term Non-Exponential Models

Two-term non-exponential model for biphasic digestion:

$$\Delta pH_t = \Delta pH_0 + \frac{t}{K_{PRP1} + K_{P2} t} + \frac{t}{K_{PRP3} + K_{P4} t} \quad (14)$$

$$\Delta pH_\infty = (\Delta pH_0 + [1/K_{P2}] + [1/K_{P4}])$$

Three-term non-exponential model for triphasic digestion:

$$\Delta pH_t = \Delta pH_0 + \frac{t}{K_{PRP1} + K_{P2} t} + \frac{t}{K_{PRP3} + K_{P4} t} + \frac{t}{K_{PRP5} + K_{P6} t} \quad (15)$$

$$\Delta pH_\infty = (\Delta pH_0 + [1/K_{P2}] + [1/K_{P4}] + [1/K_{P6}])$$

where, $1/K_{PRP1} = K_{PR1}$ = rate of digestion of phase 1, $1/K_{PRP3} = K_{PR2}$ = rate of digestion of phase 2, $1/K_{PRP5} = K_{PR3}$ = rate of digestion of phase 3, and K_{P2}, K_{P4}, and K_{P6} define maximum changes in pH (ΔpH_∞).

3.5.4. Gallagher-Corrigan Model

This is a popular model in drug release and has been applied to or reported in food digestion [53,55]:

$$\Delta pH_t = \Delta pH_1 + \Delta pH_2 [1 - \exp(-K_{PR1} t)] + \Delta pH_3 \left[\frac{\exp\{K_{PR2} (t - t_{MAX})\}}{1 + \exp\{K_{PR2} (t - t_{MAX})\}}\right]$$

$$\Delta pH_0 = \Delta pH_1 + \Delta pH_3 \left[\frac{\exp\{K_{PR2} (-t_{MAX})\}}{1 + \exp\{K_{PR2} (-t_{MAX})\}}\right]$$

$$\Delta pH_\infty = \Delta pH_1 + \Delta pH_2 + \Delta pH_3 \quad (16)$$

where ΔpH_1 = constant and t_{MAX} = time of maximum digestion rate [55]. Although the Gallagher-Corrigan model has two rates of digestion for traditional biphasic digestion, the additional parameter t_{MAX} might place it for interphases of bi- and tri-phasic digestions. It was, therefore, considered for both bi- and tri-phasic digestion modes in the present study along the lines of some models reported in Sopade [37] with one rate of digestion and an additional digestion parameter for mono- and bi-phasic digestion interphases.

Computing these models with the constraints stated above, Table 2 summarises the heterogeneity tests on the rates of digestion (K_{PR1}, K_{PR2}, K_{PR3}) from Equations (11)–(16) on the preliminary digestion modes of the genotypes and reference casein. All the models adequately described ($r^2 > 0.98$, SUMSQ ≈ 0.0, MRDM < 5.0) the genotypes and casein to show their suitability in modelling the protein digestograms with the stated constraints that ensure practical digestion parameters. The coefficients of variation (CV = 100 × standard deviation/mean) for successive

rates of digestion, $CV_{1\text{-}2}$ (phases 1 and 2) and $CV_{2\text{-}3}$ (phases 2 and 3), ranged from 17–198% to suggest substantial differences between the rates and seemingly infer multiphasic digestion modes. However, $CV_{1\text{-}2}$ and $CV_{2\text{-}3}$ are about the coefficients of variation (CV = 0 − 141%) of the mean rates of digestion (K_{PR1}, K_{PR2}, and K_{PR3}) of the genotypes. Hence, the inferred multiphasic digestion modes from $CV_{1\text{-}2}$ and $CV_{2\text{-}3}$ can only be leads and not particularly determinants of the multiphasic digestion modes. However, the $CV_{1\text{-}2}$ for the casein is generally substantially higher than the CV from its mean rates of digestion, and based on the CV test, this suggests two distinct phases of digestion with the casein. The *t*-test for the biphasic rates for the casein also returned significant differences ($p \leq 0.05$) from the segmented modified first-order kinetic model and the two-term non-exponential model to strengthen the inference of a true biphasic digestion of the casein. The *t*-test on the rates of digestion of the genotypes, however, showed no differences ($p > 0.05$) between phases 1 and 2 for the suggested or apparent biphasic digestion, and phases 1 and 2, and 2 and 3 for the suggested or apparent triphasic digestion. Finally, the 95% confidence intervals of the rates of digestion from most of the models for the genotypes overlap to suggest no phase changes, while two of the four models revealed overlapped 95% confidence intervals for the casein. From these heterogeneity indices, therefore, the pigeonpea genotypes exhibited a true monophasic digestion mode or digestogram class, homogeneous *in-vitro* proteolysis, while the reference casein is accepted to present a true biphasic digestion (Table 2). The true biphasic digestion of the casein agrees with Jin et al. [45], who used the same casein as a reference for the same pH-drop *in-vitro* protein digestion procedure. The present study is the first to detailedly establish the monophasic protein digestion in pigeonpea genotypes, non-processed or processed. This underlines the benefits of time-course *in-vitro* protein digestion in pigeonpea, more so, with plant proteins being more examined for global food and nutrition. Hence, the hypothesis that the pigeonpea genotypes in the present study are heterogeneous in *in-vitro* proteolysis is rejected, as the genotypes presented a monophasic digestion, digestion mode, or digestogram class. Practically, in the gastrointestinal tract, monophasic digestion will present one pattern of nutrient releases, while nutrient releases in multiphasic digestion will manifest in different patterns, for example, rapid and slow, to influence nutrient absorption.

3.6. Modelling Monophasic Protein Digestograms

The following kinetic models, one rate of digestion with and without an additional parameter [32,37,53], were used to model the monophasic protein digestograms of the pigeonpea genotypes to obtain their practical digestion parameters (non-linear regressions, minimal SUMSQ, and constraints). Various studies [37,56–61] have adopted examining a few *in-vitro* food digestion models to guide the choice of the most appropriate one on mechanistic and statistical (predictability) grounds. Specifically on protein digestion, Sopade and co-workers [35,45] examined exponential and non-exponential models, and they were only restricted to these models because their samples exhibited mono- and multiphasic protein digestions.

Modified first-order kinetic model, One-term exponential model

$$\Delta pH_t = \Delta pH_0 + \Delta pH_1 \left[1 - \exp\left(- K_{PR1}\, t\right)\right]$$

or

$$\Delta pH_t = \Delta pH_0 + \left(\Delta pH_\infty - \Delta pH_0\right) \left[1 - \exp\left(- K_{PR1}\, t\right)\right]$$

or

$$\Delta pH_t = \Delta pH_\infty - \Delta pH_1 \exp\left(- K_{PR1}\, t\right)$$

$$\Delta pH_\infty = \Delta pH_0 + \Delta pH_1 \quad (17)$$

Peleg Model, One-Term Non-Exponential Model

$$\Delta pH_t = \Delta pH_0 + \frac{t}{K_{PRP1} + K_{P2} t}$$

$$\left(\Delta pH_0 + [1/K_{P2}]\right) = \Delta pH_\infty$$

$$1/K_{PRP1} = K_{PR1} \quad (18)$$

Modified Paolucci-Jeanjean Model

$$\Delta pH_t = \Delta pH_0 + \left[\frac{A\,t^2}{B^2 + t^2}\right]$$

$$(\Delta pH_0 + A) = \Delta pH_\infty$$

$$1/B = K_{PR1} \quad (19)$$

where A and B are constants.

Modified Deng Model

$$\Delta pH_t = \Delta pH_\infty - \frac{\Delta pH_1}{(1 + K_{PR1}\,\Delta pH_1\,t)}$$

$$(\Delta pH_\infty - \Delta pH_1) = \Delta pH_0 \quad (20)$$

Logistic Model

$$\Delta pH_t = \frac{\Delta pH_\infty}{1 + \left(\frac{\Delta pH_\infty}{\Delta pH_0} - 1\right)\exp(-K_{PR1}\,t)} \quad (21)$$

Weibull Model

$$\Delta pH_t = \Delta pH_0 + \Delta pH_1\,(1 - \exp\,[\{-K_{PR1}\,t\}^{\beta}])$$

$$(\Delta pH_0 + \Delta pH_1) = \Delta pH_\infty \quad (22)$$

where β = shape factor.

Gompertz model

$$\Delta pH_t = \Delta pH_\infty\ \exp\left(-\exp\left[\frac{K_{PR1}\exp(1)}{\Delta pH_\infty}\{t_{LAG} - t\} + 1\right]\right)$$

$$\Delta pH_0 = \Delta pH_\infty\ \exp\left(-\exp\left[\frac{K_{PR1}\ \exp(1)\ t_{LAG}}{\Delta pH_\infty} + 1\right]\right) \quad (23)$$

where t_{LAG} = lag time

The seven models (Equations (17)–(23)) adequately ($r^2 > 0.78$; SUMSQ < 0.03; MRDM < 14.1) described the monophasic protein digestograms of the pigeonpea genotypes (Table 3), and the protein digestion parameters of the genotypes from each of the seven models were essentially not significantly ($p > 0.05$) different. This is unique because the heterogeneities in the chemical, physical, colour, and pasting properties did not significantly bear on the protein digestibility properties of the unprocessed pigeonpea genotypes. It is noteworthy that the lag factor (t_{LAG}) in the Gompertz model returned zero (0) for the genotypes to underline the absence of a lag phase and confirm the true monophasic digestion class of the pigeonpea genotypes from the Sopade Objective Procedure (Table 2). The Weibull model, however, returned values for the shape factor (β = 0.48 − 0.76) but were non-significantly ($p > 0.05$) different among the pigeonpea genotypes (varietal independence). Although some authors [55] appeared to infer multiphasic food digestion modes from the Weibull shape factor, such inference is limited and not deeply mechanistic [53]. With its four parameters, the Weibull model described the protein digestograms better (non-corrected predictability indices) than the other models with three parameters, as expected, while the modified Deng and one-term non-exponential Peleg models identically predicted the digestograms. The identical predictability indices of the latter two models for food digestograms had been observed and reported before [32,53].

Table 2. Heterogeneity test on the preliminary protein digestogram class (PDC) for the true protein digestogram class (TDC) of the Australian pigeonpea genotypes.

Sample	PDC	Critical Digestion Time (min.)		Phase 1–Digestion Rate				Phase 2–Digestion Rate				Phase 3–Digestion Rate				Phases 1-2		Phases 2-3		Predictability Indices			TDC
				Mean	CV	95% Confidence		Mean	CV	95% Confidence		Mean	CV	95% Confidence		*t*-Test	CV	*t*-Test	CV	r^2	SUMSQ	MRDM	
		Phases 1-2	Phases 2-3	(min.$^{-1}$)	(%)	Interval (min^{-1})		(min.$^{-1}$)	(%)	Interval (min^{-1})		(min.$^{-1}$)	(%)	Interval (min^{-1})		(*p* =)	(%)	(*p* =)	(%)				
						From	To			From	To			From	To								
A. Sopade Objective Procedure–Segmented Modified First-Order Kinetic Model																							
ICPL 14425	Biphasic	6.4	na	0.4	14	0.3	0.5	0.2	116	-0.1	0.4	na	na	na	na	0.20	63	na	na	0.995	0.0	2.4	**Monophasic**
ICPL 86022	Biphasic	7.6	na	0.3	50	0.1	0.5	0.1	78	0.0	0.1	na	na	na	na	0.16	97	na	na	0.996	0.0	2.7	**Monophasic**
ICPL 88039	Biphasic	7.1	na	0.3	3	0.3	0.3	0.1	123	-0.1	0.3	na	na	na	na	0.19	62	na	na	0.996	0.0	2.2	**Monophasic**
ICPL 90048	Biphasic	7.0	na	0.6	56	0.1	1.0	0.1	117	-0.1	0.3	na	na	na	na	0.20	97	na	na	0.993	0.0	2.3	**Monophasic**
ICPL 91039	Triphasic	2.3	8.6	0.7	40	0.3	1.0	0.2	45	0.1	0.4	0.3	13	0.2	0.3	0.08	64	0.46	27	0.997	0.0	2.5	**Monophasic**
ICPL 98011	Triphasic	1.5	5.8	1.7	38	0.8	2.6	0.1	129	-0.1	0.2	0.1	35	0.1	0.2	0.10	113	0.41	72	0.999	0.0	0.8	Biphasic
Casein	Biphasic	6.5	na	0.8	3	0.8	0.8	0.1	109	0.0	0.1	na	na	na	na	0.01	100	na	na	0.988	0.0	2.8	**Biphasic**
B. Two-, Three-Term Exponential Model																							
ICPL 14425	Biphasic	na	na	0.6	78	-0.1	1.3	0.1	138	-0.1	0.2	na	na	na	na	0.15	127	na	na	0.993	0.0	0.8	**Monophasic**
ICPL 86022	Biphasic	na	na	1.2	74	0.0	2.5	0.1	136	-0.1	0.2	na	na	na	na	0.15	133	na	na	0.997	0.0	1.8	**Monophasic**
ICPL 88039	Biphasic	na	na	1.6	61	0.2	2.9	0.1	8	0.1	0.2	na	na	na	na	0.14	115	na	na	0.999	0.0	0.8	Biphasic
ICPL 90048	Biphasic	na	na	1.1	61	0.2	2.0	0.0	23	0.0	0.0	na	na	na	na	0.13	135	na	na	0.996	0.0	1.9	Biphasic
ICPL 91039	Triphasic	na	na	0.5	141	-0.5	1.5	0.8	32	0.4	1.1	0.0	41	0.0	0.0	0.28	72	0.07	120	0.997	0.0	2.4	**Monophasic**
ICPL 98011	Triphasic	na	na	1.0	141	-1.0	3.0	115.5	141	-110.7	341.6	0.1	33	0.0	0.1	0.25	198	0.25	200	0.999	0.0	1.1	**Monophasic**
Casein	Biphasic	na	na	0.9	116	-0.5	2.2	0.8	123	-0.6	2.1	na	na	na	na	0.49	98	na	na	0.998	0.0	0.9	Monophasic
C. Two-, Three-Term Non-Exponential Model																							
ICPL 14425	Biphasic	na	na	500.2	141	-479.6	1,479.9	0.1	69	0.0	0.1	na	na	na	na	0.25	200	na	na	0.999	0.0	0.9	**Monophasic**
ICPL 86022	Biphasic	na	na	0.2	50	0.1	0.3	0.0	92	0.0	0.1	na	na	na	na	0.17	93	na	na	0.998	0.0	1.7	**Monophasic**
ICPL 88039	Biphasic	na	na	0.1	50	0.0	0.2	0.0	30	0.0	0.1	na	na	na	na	0.13	74	na	na	0.999	0.0	0.9	**Monophasic**
ICPL 90048	Biphasic	na	na	0.3	85	-0.1	0.7	0.0	2	0.0	0.0	na	na	na	na	0.18	141	na	na	0.994	0.0	2.7	**Monophasic**
ICPL 91039	Triphasic	na	na	0.1	138	-0.1	0.3	0.1	10	0.1	0.2	0.1	128	-0.1	0.3	0.39	71	0.36	65	0.995	0.0	3.0	**Monophasic**
ICPL 98011	Triphasic	na	na	1.1	134	-1.0	3.2	0.8	110	-0.4	1.9	0.0	6	0.0	0.0	0.29	108	0.22	162	0.999	0.0	1.1	**Monophasic**
Casein	Biphasic	na	na	1.9	12	1.6	2.2	0.0	48	0.0	0.0	na	na	na	na	0.03	113	na	na	0.997	0.0	1.1	**Biphasic**
D. Gallagher-Corrigan Model																							
ICPL 14425	Biphasic	na	na	0.7	8	0.7	0.8	0.5	3	0.5	0.5	na	na	na	na	0.07	23	na	na	0.998	0.0	1.7	Biphasic
ICPL 86022	Biphasic	na	na	0.5	27	0.3	0.7	0.5	13	0.4	0.6	na	na	na	na	0.36	17	na	na	0.998	0.0	1.8	**Monophasic**
ICPL 88039	Biphasic	na	na	0.6	29	0.3	0.8	0.5	2	0.5	0.6	na	na	na	na	0.44	17	na	na	0.999	0.0	1.2	**Monophasic**
ICPL 90048	Biphasic	na	na	0.8	66	0.1	1.6	0.8	25	0.5	1.0	na	na	na	na	0.46	42	na	na	0.999	0.0	1.2	**Monophasic**
ICPL 91039	Triphasic	na	na	17.3	138	-15.8	50.4	1.4	24	1.0	1.9	na	na	na	na	0.26	177	na	na	0.981	0.0	4.8	**Monophasic**
ICPL 98011	Triphasic	na	na	16.4	134	-14.1	46.8	0.5	4	0.5	0.6	na	na	na	na	0.25	185	na	na	0.994	0.0	2.3	**Monophasic**
Casein	Biphasic	na	na	1.2	0	1.2	1.2	0.8	44	0.3	1.2	na	na	na	na	0.16	32	na	na	0.998	0.0	1.0	Monophasic

CV = coefficient of variation, r^2 = coefficient of determination; SUMSQ = sum of squares of residuals; MRDM = mean relative deviation modulus. The recommended true digestogram classes (TDCs) are in bold. These apply wherever they appear.

Table 3. *In vitro* protein digestibility parameters from the kinetic models for monophasic digestion mode of the Australian pigeonpea genotypes.

Parameter	ICPL 14425	ICPL 86022	ICPL 88039	ICPL 90048	ICPL 91039	ICPL 98011
A. Gompertz model (r^2 > 0.855; SUMSQ < 0.030; MRDM < 14.1)						
ΔpH_0	0.03 ± 0.00 [a]	0.02 ± 0.00 [a]	0.02 ± 0.00 [a]	0.02 ± 0.00 [a]	0.02 ± 0.00 [a]	0.02 ± 0.00 [a]
ΔpH_∞	0.39 ± 0.06 [a]	0.37 ± 0.05 [a]	0.29 ± 0.01 [a]	0.32 ± 0.00 [a]	0.35 ± 0.02 [a]	0.33 ± 0.04 [a]
t_{LAG}	0.0 ± 0.0	0.0 ± 0.0	0.0 ± 0.0	0.0 ± 0.0	0.0 ± 0.0	0.0 ± 0.0
$K_{PR1} \times 10^{-3}$	94.7 ± 4.5 [a]	81.0 ± 35.5 [a]	59.8 ± 2.2 [a]	99.5 ± 49.1 [a]	116.9 ± 61.9 [a]	70.8 ± 13.0 [a]
$IVPD_{10min.}$	72.7 ± 1.0 [a]	72.2 ± 0.9 [a]	70.9 ± 0.2 [a]	71.4 ± 0.0 [a]	72.0 ± 0.3 [a]	71.5 ± 0.7 [a]
B. Logistic model (r^2 > 0.802; SUMSQ < 0.021; MRDM < 10.6)						
ΔpH_0	0.08 ± 0.01 [a]	0.07 ± 0.02 [a]	0.05 ± 0.00 [a]	0.08 ± 0.03 a	0.06 ± 0.00 [a]	0.08 ± 0.03 [a]
ΔpH_∞	0.40 ± 0.06 [a]	0.37 ± 0.05 [a]	0.29 ± 0.01 [a]	0.33 ± 0.01 [a]	0.35 ± 0.01 [a]	0.35 ± 0.05 [a]
$K_{PR1} \times 10^{-3}$	625.0 ± 31.3 [a]	615.2 ± 112.5 [a]	600.1 ± 34.6 [a]	610.9 ± 66.8 [a]	978.6 ± 478.2 [a]	465.0 ± 71.9 [a]
$IVPD_{10min.}$	72.8 ± 1.0 [a]	72.3 ± 1.0 [a]	70.9 ± 0.2 [a]	71.7 ± 0.2 [a]	72.0 ± 0.3 [a]	71.8 ± 0.9 [a]
C. Modified Deng model (r^2 > 0.957; SUMSQ < 0.008; MRDM < 6.2)						
ΔpH_0	0.01 ± 0.01 [abc]	0.01 ± 0.01 [ab]	0.01 ± 0.01 [abc]	0.00 ± 0.00 [abc]	0.04 ± 0.02 [b]	0.08 ± 0.03 [a]
ΔpH_∞	0.56 ± 0.03 [a]	0.44 ± 0.01 [a]	0.45 ± 0.07 [a]	0.47 ± 0.05 [a]	0.50 ± 0.06 [a]	0.35 ± 0.05 [a]
$K_{PR1} \times 10^{-3}$	450.0 ± 299.8 [a]	504.0 ± 4.2 [a]	993.3 ± 804.9 [a]	1,194.6 ± 982.3 [a]	412.7 ± 40.5 [a]	465.0 ± 71.9 [a]
$IVPD_{10min.}$	73.1 ± 1.1 [a]	72.6 ± 1.1 [a]	71.2 ± 0.2 [a]	71.8 ± 0.1 [a]	72.4 ± 0.4 [a]	71.9 ± 0.8 [a]
D. Modified first-order kinetic model, One-term exponential model (r^2 > 0.927; SUMSQ < 0.012; MRDM < 7.3)						
ΔpH_0	0.03 ± 0.00 [a]	0.02 ± 0.00 [a]	0.02 ± 0.01 [a]	0.03 ± 0.02 [a]	0.01 ± 0.00 [a]	0.05 ± 0.03 [a]
ΔpH_∞	0.43 ± 0.07 [a]	0.42 ± 0.02 [a]	0.33 ± 0.01 [a]	0.36 ± 0.02 [a]	0.38 ± 0.00 [a]	0.39 ± 0.06 [a]
$K_{PR1} \times 10^{-3}$	287.3 ± 34.8 [a]	251.7 ± 110.1 [a]	240.5 ± 9.5 [a]	320.0 ± 131.4 [a]	440.4 ± 251.0 [a]	202.2 ± 17.3 [a]
$IVPD_{10min.}$	73.0 ± 1.1 [a]	72.5 ± 1.0 [a]	71.1 ± 0.2 [a]	71.8 ± 0.1 [a]	72.2 ± 0.3 [a]	71.9 ± 0.8 [a]
E. Modified Paolucci-Jeanjean model (r^2 > 0.783; SUMSQ < 0.018; MRDM < 9.4)						
ΔpH_0	0.07 ± 0.01 [a]	0.05 ± 0.00 [a]	0.04 ± 0.01 [a]	0.05 ± 0.00 [a]	0.03 ± 0.01 [a]	0.08 ± 0.03 [a]
ΔpH_∞	0.42 ± 0.07 [a]	0.39 ± 0.04 [a]	0.31 ± 0.01 [a]	0.34 ± 0.01 [a]	0.37 ± 0.01 [a]	0.37 ± 0.06 [a]
$K_{PR1} \times 10^{-3}$	387.8 ± 45.2 [a]	369.3 ± 146.1 [a]	332.7 ± 14.7 [a]	519.1 ± 258.5 [a]	612.8 ± 335.3 [a]	279.6 ± 33.0 [a]
$IVPD_{10min.}$	72.8 ± 1.0 [a]	72.3 ± 1.0 [a]	70.9 ± 0.2 [a]	71.5 ± 0.1 [a]	72.1 ± 0.4 [a]	71.7 ± 0.8 [a]
F. Peleg model, One-term non-exponential model (r^2 > 0.957; SUMSQ < 0.008; MRDM < 6.2)						
ΔpH_0	**0.02 ± 0.00 [a]**	**0.01 ± 0.01 [a]**	**0.01 ± 0.01 [a]**	**0.01 ± 0.01 [a]**	**0.00 ± 0.00 [a]**	**0.04 ± 0.02 [a]**
ΔpH_∞	**0.55 ± 0.11 [a]**	**0.56 ± 0.03 [a]**	**0.44 ± 0.01 [a]**	**0.45 ± 0.07 [a]**	**0.47 ± 0.05 [a]**	**0.50 ± 0.06 [a]**
$K_{PR1} \times 10^{-3}$	**153.3 ± 1.4 [a]**	**134.9 ± 81.2 [a]**	**93.6 ± 7.9 [a]**	**166.3 ± 93.0 [a]**	**238.4 ± 161.5 [a]**	**89.6 ± 3.8 [a]**
$IVPD_{10min.}$	**73.1 ± 1.1 [a]**	**72.6 ± 1.1 [a]**	**71.2 ± 0.2 [a]**	**71.8 ± 0.1 a**	**72.4 ± 0.4 [a]**	**71.9 ± 0.8 [a]**
G. Weibull model (r^2 > 0.983; SUMSQ < 0.003; MRDM < 5.2)						
ΔpH_0	0.00 ± 0.00 [a]	0.00 ± 0.00 [a]	0.00 ± 0.00 [a]	0.00 ± 0.00 [a]	0.00 ± 0.00 [a]	0.00 ± 0.01 [a]
ΔpH_∞	0.60 ± 0.10 [a]	0.56 ± 0.05 [a]	0.43 ± 0.05 [a]	3.27 ± 3.87 [a]	0.42 ± 0.04 [a]	3.72 ± 3.23 [a]
β	0.62 ± 0.03 [a]	0.72 ± 0.03 [a]	0.73 ± 0.09 [a]	0.51 ± 0.26 [a]	0.76 ± 0.03 [a]	0.48 ± 0.06 [a]
$K_{PR1} \times 10^{-3}$	136.1 ± 16.7 [a]	150.6 ± 99.4 [a]	146.6 ± 55.3 [a]	52.3 ± 73.9 [a]	388.0 ± 286.4 [a]	3.7 ± 5.0 [a]
$IVPD_{10min.}$	73.3 ± 1.1 [a]	72.7 ± 1.1 [a]	71.2 ± 0.2 [a]	72.1 ± 0.3 [a]	72.4 ± 0.3 [a]	72.0 ± 0.7 [a]

The Peleg model, the one-term non-exponential model, (bold) is recommended for the genotypes. The units of t_{LAG}, K_{PR1}, and $IVPD_{10min.}$ are min., $min.^{-1}$, and % respectively.

With the two-term non-exponential model and the segmented modified first-order kinetic model suitably predicting the biphasic digestion of the reference casein (Table 2), further analysis of the monophasic protein digestograms of the pigeonpea genotypes was based on the Peleg model, the one-term non-exponential model (Equation (18)). This is because Table 3 shows that the Peleg model, the one-term non-exponential model (Equation (18)), predicted the digestograms of the pigeonpea genotypes better than the modified first-order kinetic model, the one-term exponential model (Equation (17)). Moreover, Equation (18) is the foundation of the two-term non-exponential model (Equation (14)), which incidentally predicted the protein digestograms of the reference casein better (Table 2 and Supplementary Figure S2) than the segmented modified first-order kinetic model (Equation (11)). Equation (18) is, therefore, appropriate and recommended for the genotypes, while Equation (14) is suitable and recommended to model the reference casein. This ensures model consistency (one- and two-term non-exponential models) in the study. Sopade [32] recommended model consistency, wherever possible or appropriate, if and when both mono- and multi-phasic digestograms or digestion modes were established in a study. As discussed above, Jin et al. [45] and Li and Sopade [35] adopted this approach to better understand their samples.

Figure 3 shows how the Peleg (one-term exponential) model adequately described the monophasic digestograms of the pigeonpea genotypes, and the predicted parameters (Table 3, bold) showed no significant ($p > 0.05$) differences among the samples, like the protein digestion parameters discussed above. Some of the parameters revealed high CV, which might question the suitability of the model. In addition to the predictability indices in Table 3, the residual plots from the model (Figure 3) and others (not shown) were investigated with the Quantile-Quantile (Q-Q) plots [53,62,63] to objectively and quantitatively ascertain patterned or non-patterned residuals. Acceptable non-patterned residuals follow a normal distribution, present a uniform band around zero, and define identical data and theoretical coefficients, vis-à-vis slope = 1.0 and intercept = 0, and a non-significant X^2-test in the Q-Q plots [53,64]. With the X^2-test revealing non-significance ($p > 0.05$) and consequently, non-patterned residuals in the duplicates and averages (the Q-Q plots in Figure 3 for thoroughness), the Peleg model is a confirmed recommendation to describe the *in-vitro* protein digestion of the pigeonpea genotypes. The modelling and thorough evaluation of the reference casein are in Supplementary Figures S2 and S3, and the resulting $IVPD_{10min}$. and area under the digestogram of the casein are of the same order as the values for the casein in Jin et al. [45], even though Jin et al. [45] described the *in-vitro* protein digestogram of the casein with the two-term exponential model (Equation (12)).

Relative to casein as a reference in proteolysis, Sopade and co-workers [35,45] discussed the hydrolysis index in proteolysis ($HI_{PROTEIN}$) to better examine nutrient asynchrony when compared with the hydrolysis index in amylolysis. There is a potential for a hydrolysis index in lipolysis, lipid digestion, when a universal lipid reference is identified, analysed, and standardised to complete hydrolysis indices for the three macromolecules or macronutrients. With differences in *in-vitro* digestion protocols, hydrolysis indices are universal, unlike rates of digestion from different protocols. The need to standardise protein digestibility studies from different methods continues to be emphasised [24,32], and $HI_{PROTEIN}$ offers a universal option. $HI_{PROTEIN}$ (area under the sample digestogram/area under casein digestogram) in proteolysis was examined [35,45] for processed and non-processed samples and used to predict *in-vitro* protein digestibility (pIVPD). Figure 4 shows the area under the sample digestogram (AUC), $HI_{PROTEIN}$, pIVPD (Equation [9]), and $IVPD_{AVG}$ (Equation [10]) for the genotypes. The integrals of the one- and two-term non-exponential models in Sopade [37,60] were used to calculate the areas under the digestograms of the pigeonpea genotypes and casein. These useful protein digestion parameters were non-significantly ($p > 0.05$) different among the pigeonpea genotypes, further underlining their homogeneity in *in-vitro* proteolysis. In essence, the heterogeneous unprocessed pigeonpea genotypes revealed homogeneous *in-vitro* proteolysis. It is recognised that food processing can differently affect proteolysis with structural responses that can define each different *in-vitro* proteolysis. So, homogeneous *in-vitro* proteolysis in unprocessed samples might be retained or modified by food processes, and this needs to be established for pigeonpea in processed (more) and non-processed formulations.

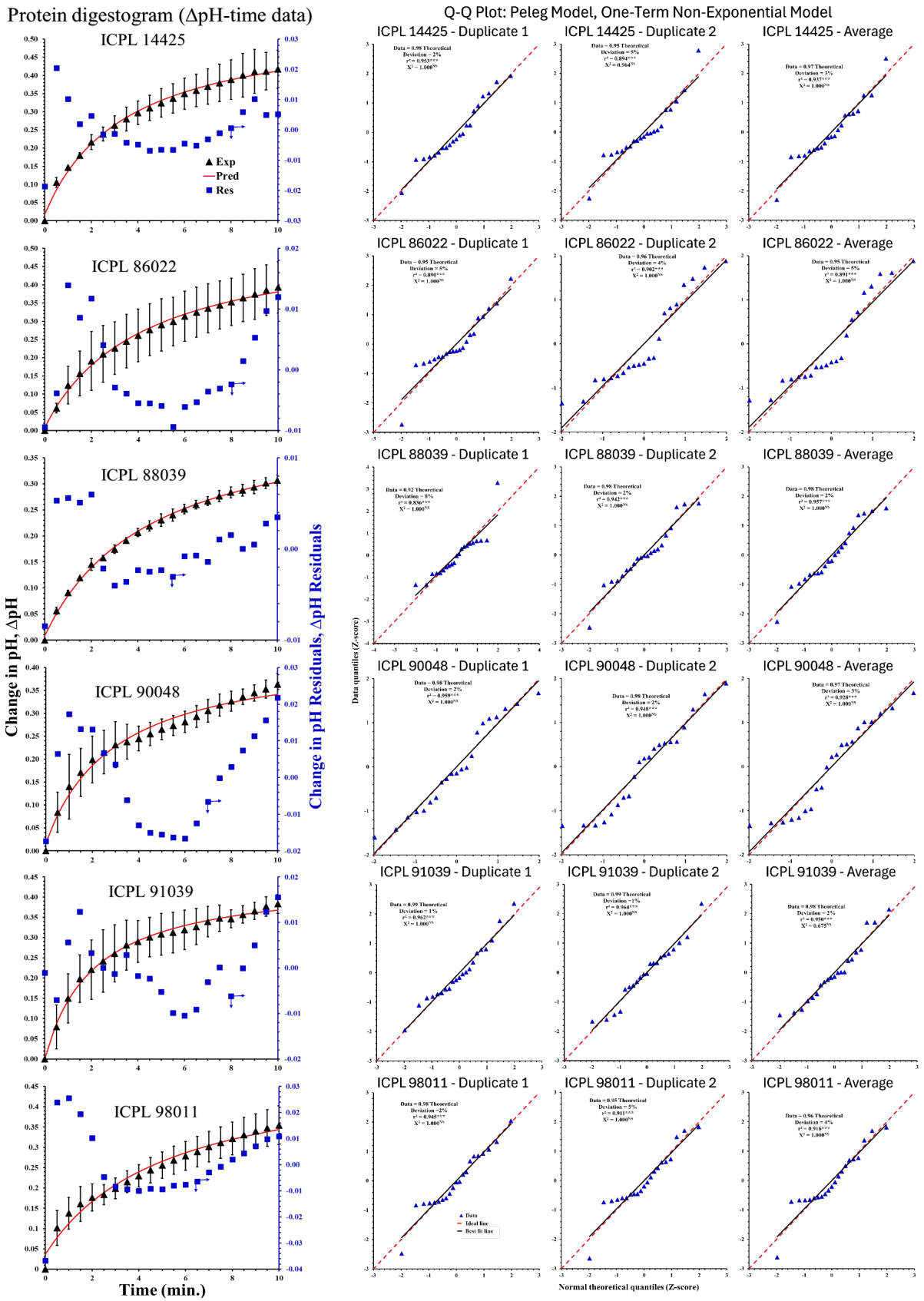

Figure 3. Protein digestograms of the pigeonpea genotypes modelled with the Peleg (one-term non-exponential) model.

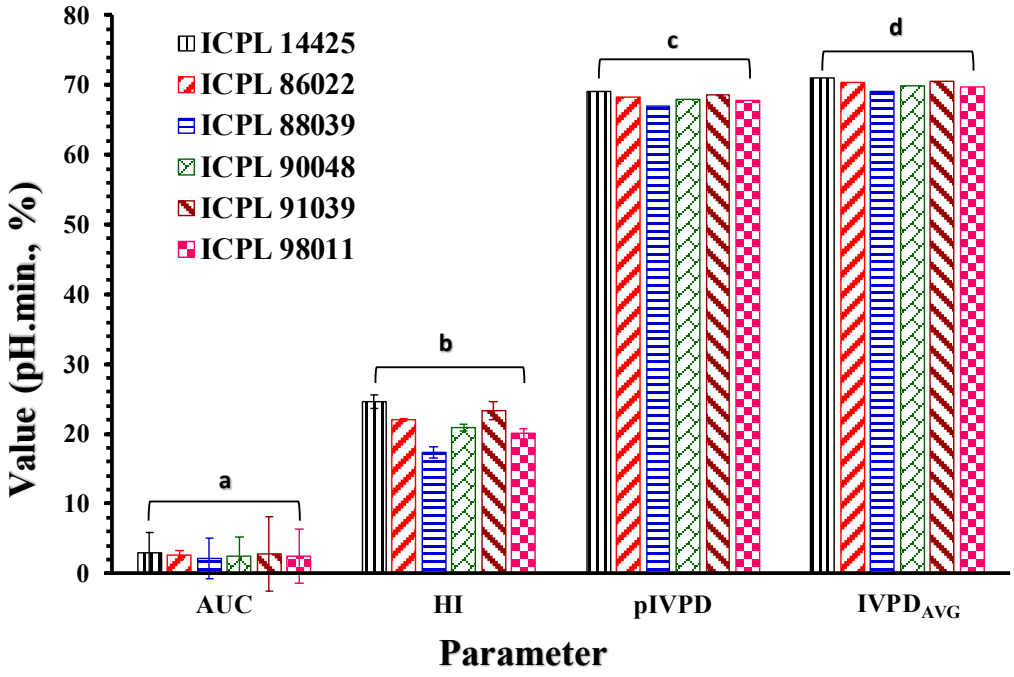

Figure 4. Additional protein digestion parameters of the pigeonpea genotypes from the Peleg (one-term non-exponential) model (AUC = Area under digestogram, pH.min.; HI = Hydrolysis index, %; pVPD = Predicted *in-vitro* protein digestibility, %; $IVPD_{AVG}$ = Average *in-vitro* protein digestibility, %). For each parameter, bar charts with the same figure show non-significance ($p > 0.05$).

4. Conclusions

With pigeonpea, a potential contributor to the growing global plant protein industry, six Australian genotypes from a global pigeonpea line were investigated for their chemical, physical, colour, pasting, and protein digestibility properties. The genotypes were heterogeneous in these properties, except their protein digestion, which revealed a homogeneous monophasic digestion mode, with digestion parameters that were not significantly different among the genotypes. The hypothesis of heterogeneous food properties of the pigeonpea genotypes is, therefore, rejected.

The protein digestibilities of the pigeonpea genotypes were investigated in detail using objective procedures for statistical and mechanistic confidence in the deduced digestion mode. With rates of digestion defining nutrient releases and availabilities in the gastro-intestinal tract, the present study pioneers kinetics of protein digestion in pigeonpea to detailedly establish the digestion mode. Amongst the seven kinetic modes for monophasic protein digestion investigated, the Peleg model, a one-term non-exponential model, is recommended for the pigeonpea genotypes. This study opens guidelines for *in-vitro* proteolysis of pigeonpea and generally plant proteins for useful information that solidifies the global plant protein industry.

Supplementary Materials

The additional data and information can be downloaded at: https://media.sciltp.com/articles/others/2605221003448976/FSP-26020118-MS.pdf.

Author Contributions

D.M.: investigation, data curation, formal analysis, writing—original draft preparation; P.A.S.: conceptualization, methodology, software, supervision, investigation, data curation, formal analysis, writing—original draft preparation, visualization, validation, writing—reviewing and editing. All authors have read and agreed to the published version of the manuscript.

Funding

This research received no external funding.

Institutional Review Board Statement

Not applicable.

Informed Consent Statement

Not applicable.

Data Availability Statement

Data are available upon reasonable request.

Acknowledgments

Part of this study was conducted in 2013 at The University of Queensland, Brisbane, Australia, and the pigeonpea were obtained from the Queensland Department of Primary Industries, Kingaroy, Australia (through Professor RCN Rachaputi). The authors are grateful.

Conflicts of Interest

The authors declare no conflict of interest.

Use of AI and AI-Assisted Technologies

No AI tools were utilized for this paper.

References

1. Fasoyiro, S.B.; Ajibade, S.R.; Saka, J.O.; et al. Physical Characteristics and Effects of Processing Methods on Pigeon Pea Varieties. *J. Food Agric. Environ.* **2002**, *3*, 59–61.
2. Chauhan, Y.; Krosch, S.; Sands, D.; et al. Agronomic Characteristics of Pigeonpea as a Summer Crop for Queensland. In Proceedings of the 20th Australian Agronomy Conference, Toowoomba, QLD, Australia, 18–22 September 2022.
3. Locali-Pereira, A.R.; Boire, A.; Berton-Carabin, C.; et al. Pigeon Pea, an Emerging Source of Plant-Based Proteins. *ACS Food Sci. Technol.* **2023**, *3*, 1777–1799. https://doi.org/10.1021/acsfoodscitech.3c00268.
4. Wu, J.; Zhou, Q.; Zhou, C.; et al. Strategies to Promote the Dietary Use of Pigeon Pea (*Cajanus cajan* L.) for Human Nutrition and Health. *Food Front.* **2024**, *5*, 1014–1030. https://doi.org/10.1002/fft2.381.
5. Haji, A.; Teka, T.A.; Bereka, T.Y.; et al. Nutritional Composition, Bioactive Compounds, Food Applications, and Health Benefits of Pigeon Pea (*Cajanus cajan* L. Millsp.): A Review. *Legume Sci.* **2024**, *6*, e233. https://doi.org/10.1002/leg3.233.
6. Food and Agriculture Organization of the United Nations. Available online: https://www.fao.org/faostat/en/#data/QCL (accessed on 12 November 2025).
7. Benítez, R.B.; Tabares, W.F.E.; Velásquez, L.A.L.; et al. Enzymatic Hydrolysis as a Tool to Improve Total Digestibility and Techno-Functional Properties of Pigeon Pea (*Cajanus cajan*) Starch. *Heliyon* **2021**, *7*, e07817. https://doi.org/10.1016/j.heliyon.2021.e07817.
8. Kumari, B.; Sit, N. Physicochemical, Rheological Properties, and in-Vitro Starch Digestibility of Flours and Starches from Pigeon Pea, Cowpea, Pinto Bean, and Navy Bean. *Starch Stärke* **2024**, *76*, 2300303. https://doi.org/10.1002/star.202300303.
9. Sultana, R.; Vales, M.I.; Saxena, K.B.; et al. Waterlogging Tolerance in Pigeonpea (*Cajanus cajan* (L.) Millsp.): Genotypic Variability and Identification of Tolerant Genotypes. *J. Agric. Sci.* **2013**, *151*, 659–671. https://doi.org/10.1017/S0021859612000755.
10. Kachare, D.P.; Satbhai, R.D.; Rathod, D.B.; et al. Evaluation of Pigeon Pea (*Cajanus cajan* L.) Genotypes for Nutritional Quality. *Legume Res.* **2017**, *42*, 485–489. https://doi.org/10.18805/LR-3899.
11. Ravika, Y.; Yadav, R.; Kumari, N.; et al. Genetic Diversity for Quality Traits and Seed Yield in Pigeonpea [*Cajanus cajan* (L.) Millsp.]. *Int. J. Curr. Microbiol. Appl. Sci.* **2019**, *8*, 2837–2844. https://doi.org/10.20546/ijcmas.2019.806.342.
12. Anon. Legumes Program: Quarterly Technical Report—January–March 1993. Available online: https://oar.icrisat.org/8175/1/RP%208228.pdf (accessed on 12 November 2025).
13. Tiwari, A.; Singh, P.; Maurya, C.L.; et al. Assessment of Nutritional Attributes in Pigeonpea Genotypes: Protein Quality, Carbohydrate Fractions, and Digestibility Patterns. *Int. J. Adv. Biochem. Res.* **2025**, *9*, 4–9. https://doi.org/10.33545/26174693.2025.v9.i9Sa.5461.
14. Yohane, E.N.; Shimelis, H.; Laing, M.; et al. Genotype-by-Environment Interaction and Stability Analyses of Grain Yield in Pigeonpea [*Cajanus cajan* (L.) Millspaugh]. *Acta Agric. Scand. B Soil Plant Sci.* **2021**, *71*, 145–155. https://doi.org/10.1080/09064710.2020.1859608.

15. Legume Varieties Released by UQ Will Increase Volume for Local Growers. Available online: https://afdj.com.au/legume-varieties-released-by-uq-will-increase-volume-for-local-growers/ (accessed on 12 November 2025).
16. Singh, A.K.; Elango, D.; Raigne, J.; et al. Plant-Based Protein Crops and Their Improvement: Current Status and Future Perspectives. *Crop Sci.* **2025**, *65*, e21389. https://doi.org/10.1002/csc2.21389.
17. Anyiam, P.N.; Phongthai, S.; Pongsetkul, J.; et al. Novel-Assisted Extraction Methods for Protein Recovering from Bambara Groundnut: Composition, Techno-Functional and Digestibility. *J. Food Biochem.* **2026**, *2026*, 6622287. https://doi.org/10.1155/jfbc/6622287.
18. Ohanenye, I.C.; Sun, X.; Sarteshnizi, R.A.; et al. Germination Alters the Microstructure, *in Vitro* Protein Digestibility, α-Glucosidase and Dipeptidyl Peptidase-IV Inhibitory Activities of Bioaccessible Fraction of Pigeon Pea (*Cajanus cajan*) Seeds. *Legume Sci.* **2021**, *3*, e79. https://doi.org/10.1002/leg3.79.
19. Rizvi, Q.U.E.H.; Kumar, K.; Ahmed, N.; et al. Influence of Soaking and Germination Treatments on the Nutritional, Anti-Nutritional, and Bioactive Composition of Pigeon Pea (*Cajanus cajan* L.). *J. Appl. Biol. Biotechnol.* **2022**, *10*, 127–134. https://doi.org/10.7324/JABB.2022.100317.
20. Mahendraraj, S.; Collins, M.; Chauhan, Y.; et al. Reliability of Nonlinear Least Square Broken Stick Model in Quantifying the Effects of Temperature and Photoperiod on Flowering of Pigeonpea Genotypes (*Cajanus cajan* (L.) Millsp.). *J. Appl. Nat. Sci.* **2024**, *16*, 502–508. https://doi.org/10.31018/jans.v16i2.4840.
21. Winter, B. Pigeonpea: A New Dryland Summer Pulse for Northern Region Farming Systems. Available online: https://grdc.com.au/resources-and-publications/grdc-update-papers/tab-content/grdc-update-papers/2024/07/pigeonpea-a-new-dryland-summer-pulse-for-northern-region-farming-systems (accessed on 12 November 2025).
22. Oluwole, O.B.; Nicholas-Okpara, V.A.N.; Elemo, G.; et al. Medicinal Uses, Nutraceutical Potentials, and Traditional Farm Production of Bambara Beans and Pigeon Peas. *Glob. J. Epidemiol. Public Health* **2022**, *20*, 41–50. https://doi.org/10.12974/2313-0946.2021.06.01.3.
23. Chinma, C.E.; Abu, J.O.; Adedeji, O.E.; et al. Nutritional Composition, Bioactivity, Starch Characteristics, Thermal and Microstructural Properties of Germinated Pigeon Pea Flour. *Food Biosci.* **2022**, *49*, 101900. https://doi.org/10.1016/j.fbio.2022.101900.
24. Ohanenye, I.C.; Ekezie, F.-G. C.; Sarteshnizi, R.A.; et al. Legume Seed Protein Digestibility as Influenced by Traditional and Emerging Physical Processing Technologies. *Foods* **2022**, *11*, 2299. https://doi.org/10.3390/foods11152299.
25. Opazo-Navarrete, M.; Burgos-Díaz, C.; Bravo-Reyes, C.; et al. Comprehensive Review of Plant Protein Digestibility: Challenges, Assessment Methods, and Improvement Strategies. *Appl. Sci.* **2025**, *15*, 3538. https://doi.org/10.3390/app15073538.
26. Lao, Y.; Ye, Q.; Wang, Y.; et al. Modulating Digestibility and Mitigating Beany Flavor of Pea Protein. *Food Rev. Int.* **2024**, *40*, 3129–3158. https://doi.org/10.1080/87559129.2024.2346329.
27. Sharma, S.; Singh, A.; Singh, B. Characterization of *in Vitro* Antioxidant Activity, Bioactive Components, and Nutrient Digestibility in Pigeon Pea (*Cajanus cajan*) as Influenced by Germination Time and Temperature. *J. Food Biochem.* **2019**, *43*, e12706. https://doi.org/10.1111/jfbc.12706.
28. Dutta, M.; Dineshkumar, R.; Nagesh, C.R.; et al. Exploring Protein Structural Adaptations and Polyphenol Interactions: Influences on Digestibility in Pigeon Pea Dal and Whole Grains under Heat and Germination Conditions. *Food Chem.* **2024**, *460*, 140561. https://doi.org/10.1016/j.foodchem.2024.140561.
29. Thomas, D.J.; Lu, Z.; Brummer, Y.; et al. Assessment of Protein Quality and Nutritional Characteristics of Commonly Consumed Pulses in the Caribbean Diet by Different *in Vitro* Assays. *Foods* **2025**, *14*, 283. https://doi.org/10.3390/foods14020283.
30. Mackie, A. Insights and Gaps on Protein Digestion. *Curr. Opin. Food Sci.* **2020**, *31*, 96–101. https://doi.org/10.1016/j.cofs.2020.03.006.
31. Sousa, R.; Portmann, R.; Dubois, S.; et al. Protein Digestion of Different Protein Sources Using the INFOGEST Static Digestion Model. *Food Res. Int.* **2020**, *130*, 108996. https://doi.org/10.1016/j.foodres.2020.108996.
32. Sopade, P.A. Computational Characteristics of Kinetic Models for *in Vitro* Protein Digestion: A Review. *J. Food Eng.* **2024**, *360*, 111690. https://doi.org/10.1016/j.jfoodeng.2023.111690.
33. Nguyen, G.T.; Sopade, P.A. Modeling Starch Digestograms: Computational Characteristics of Kinetic Models for *in Vitro* Starch Digestion in Food Research. *Compr. Rev. Food Sci. Food Saf.* **2018**, *17*, 1422–1445. https://doi.org/10.1111/1541-4337.12384.
34. Verkempinck, S.H.E.; Duijsens, D.; Michels, D.; et al. Studying Semi-Dynamic Digestion Kinetics of Food: Establishing a Computer-Controlled Multireactor Approach. *Food Res. Int.* **2022**, *156*, 111301. https://doi.org/10.1016/j.foodres.2022.111301.
35. Li, Y.; Sopade, P.A. Kinetics of *in Vitro* Protein Digestion in an Extruded Model Sorghum-Barley Blend: Processing and Property Relationships. *J. Food Eng.* **2025**, *391*, 112437. https://doi.org/10.1016/j.jfoodeng.2024.112437.

36. Mahasukhonthachat, K.; Sopade, P.A.; Gidley, M.J. Kinetics of Starch Digestion in Sorghum as Affected by Particle Size. *J. Food Eng.* **2010**, *96*, 18–28. https://doi.org/10.1016/j.jfoodeng.2009.06.051.
37. Sopade, P.A. Homogeneities in *in Vitro* Starch Digestion of Compositionally Heterogenous White Wheat Breads. *Int. J. Food Sci. Technol.* **2022**, *57*, 4380–4391. https://doi.org/10.1111/ijfs.15766.
38. Nguyen, G.T.; Gidley, M.J.; Sopade, P.A. Dependence of *in Vitro* Starch and Protein Digestions on Particle Size of Field Peas (*Pisum sativum* L.). *LWT Food Sci. Technol.* **2015**, *63*, 541–549. https://doi.org/10.1016/j.lwt.2015.03.037.
39. Koa, S.S.; Jin, X.; Zhang, J.; et al. Extrusion of a Model Sorghum-Barley Blend: Starch Digestibility and Associated Properties. *J. Cereal Sci.* **2017**, *75*, 314–323. https://doi.org/10.1016/j.jcs.2017.04.007.
40. Waramboi, J.G.; Dennien, S.; Gidley, M.J.; et al. Characterization of Sweetpotato from Papua New Guinea and Australia: Physicochemical, Pasting and Gelatinization Properties. *Food Chem.* **2011**, *126*, 1759–1770. https://doi.org/10.1016/j.foodchem.2010.12.077.
41. Uriarte-Aceves, P.M.; Rangel-Peraza, J.G.; Sopade, P.A. Kinetics of Water Absorption and Relation with Physical, Chemical, and Wet-Milling Properties of Commercial Yellow Maize (*Zea mays* L.) Hybrids. *J. Food Process. Preserv.* **2020**, *44*, e14509. https://doi.org/10.1111/jfpp.14509.
42. Uriarte-Aceves, P.M.; Sopade, P.A.; Rangel-Peraza, J.G. Physical, Chemical and Wet-Milling Properties of Commercial White Maize Hybrids Cultivated in México. *J. Food Process. Preserv.* **2019**, *43*, e13998. https://doi.org/10.1111/jfpp.13998.
43. Hsu, H.W.; Vavak, D.L.; Satterlee, L.D.; et al. A Multienzyme Technique for Estimating Protein Digestibility. *J. Food Sci.* **1977**, *42*, 1269–1273. https://doi.org/10.1111/j.1365-2621.1977.tb14476.x.
44. Tinus, T.; Damour, M.; van Riel, V.; et al. Particle Size-Starch-Protein Digestibility Relationships in Cowpea (*Vigna unguiculata*). *J. Food Eng.* **2012**, *113*, 254–264. https://doi.org/10.1016/j.jfoodeng.2012.05.041.
45. Jin, X.; Li, Y.; Koa, S.S.; et al. *In Vitro* Protein and Starch Digestibilities of Multigrain Sorghum-Barley Mixtures. *J. Food Eng.* **2024**, *379*, 112135. https://doi.org/10.1016/j.jfoodeng.2024.112135.
46. Bera, I.; O'Sullivan, M.; Flynn, D.; et al. Relationship between Protein Digestibility and the Proteolysis of Legume Proteins during Seed Germination. *Molecules* **2023**, *28*, 3204. https://doi.org/10.3390/molecules28073204.
47. Burstin, J.; Gallardo, K.; Mir, R.R.; et al. Improving Protein Content and Nutrition Quality. In *Biology and Breeding of Food Legumes*; Pratap, A., Kumar, J., Eds.; CABI: Wallingford, UK, 2011; pp. 314–328.
48. Oloyo, R.A. Chemical and Nutritional Quality Changes in Germinating Seeds of *Cajanus cajan* L. *Food Chem.* **2004**, *85*, 497–502. https://doi.org/10.1016/S0308-8146(02)00454-5.
49. Sangronis, E.; Machado, C. Influence of Germination on the Nutritional Quality of *Phaseolus vulgaris* and *Cajanus cajan*. *LWT Food Sci. Technol.* **2007**, *40*, 116–120. https://doi.org/10.1016/j.lwt.2005.08.003.
50. Singh, U.; Rao, P.V.; Subrahmanyam, N.; et al. Cooking Characteristics, Chemical Composition and Protein Quality of Newly Developed Genotypes of Pigeonpea (*Cajanus cajan* L). *J. Sci. Food Agric.* **1993**, *61*, 395–400. https://doi.org/10.1002/jsfa.2740610404.
51. Mihalyi, E.; Billick, I.H. Transformation of Fibrinogen into Fibrin III. Kinetics of the pH Change Associated with the Clotting of Fibrinogen. *Biochim. Biophys. Acta* **1963**, *71*, 97–108. https://doi.org/10.1016/0006-3002(63)90989-2.
52. Mihalyi, E.; Godfrey, J.E. Kinetic Studies of the Digestion of Fibrinogen by α-Chymotrypsin. *Biochim. Biophys. Acta* **1967**, *132*, 94–103. https://doi.org/10.1016/0005-2744(67)90195-7.
53. Sopade, P.A. Computational Characteristics of Kinetic Models for Lipolysis: Part I—Models with One Rate of Digestion for Monophasic *in Vitro* Lipid Digestograms. *Eur. Food Res. Technol.* **2026**, *252*, 148. https://doi.org/10.1007/s00217-026-05072-1.
54. Gallagher, K.M.; Corrigan, O.I. Mechanistic Aspect of the Release of Levamisole Hydrochloride from Biodegradable Polymers. *J. Control. Release* **2000**, *69*, 261–272. https://doi.org/10.1016/S0168-3659(00)00305-9.
55. González, C.; Simpson, R.; Vega, O.; et al. Effect of Particle Size on *in Vitro* Intestinal Digestion of Emulsion-Filled Gels: Mathematical Analysis Based on the Gallagher–Corrigan Model. *Food Bioprod. Process.* **2020**, *120*, 33–40. https://doi.org/10.1016/j.fbp.2019.12.009.
56. Aleixandre, A.; Benavent-Gil, Y.; Moreira, R.; et al. *In Vitro* Digestibility of Gels from Different Starches: Relationship between Kinetic Parameters and Microstructure. *Food Hydrocoll.* **2021**, *120*, 106909. https://doi.org/10.1016/j.foodhyd.2021.106909.
57. Barua, S.; Rakshit, M.; Srivastav, P.P. Optimization and Digestogram Modeling of Hydrothermally Modified Elephant Foot Yam (*Amorphophallus paeoniifolius*) Starch Using Hot Air Oven, Autoclave, and Microwave Treatments. *LWT Food Sci. Technol.* **2021**, *145*, 111283. https://doi.org/10.1016/j.lwt.2021.111283.
58. Barua, S.; Tudu, K.; Rakshit, M.; et al. Characterization and Digestogram Modeling of Modified Elephant Foot Yam (*Amorphophallus paeoniifolius*) Starch Using Ultrasonic Pretreated Autoclaving. *J. Food Process Eng.* **2021**, *144*, e13841. https://doi.org/10.1111/jfpe.13841.

59. Mahajan, P.; Bera, M.B.; Panesar, P.S. Structural, Functional, Textural Characterization and *in Vitro* Digestibility of Underutilized Kutki Millet (*Panicum sumatrense*) Starch. *LWT Food Sci. Technol.* **2022**, *154*, 112831. https://doi.org/10.1016/j.lwt.2021.112831.
60. Sopade, P.A. Modelling Multiphasic Starch Digestograms with Multiterm Exponential and Non-Exponential Equations. *Carbohydr. Polym.* **2022**, *275*, 118698. https://doi.org/10.1016/j.carbpol.2021.118698.
61. Saraswat, S.; Mahajan, P.; Bera, M.B. Comparative Evaluation of Structural, Functional, Textural Characterization, and *in Vitro* Digestibility of Native and Physically Modified Kodo Millet (*Paspalum scrobiculatum*) Starch. *Food Sci. Biotechnol.* **2026**. https://doi.org/10.1007/s10068-026-02094-z.
62. Castillo-Gutiérrez, S.; Estudillo-Martínez, M.D.; Lozano-Aguilera, E.D. Influence of the Fitted Straight Line for Confidence Bands Algorithm in Q-Q Plots. *Open J. Stat.* **2021**, *11*, 925–930. https://doi.org/10.4236/ojs.2021.116054.
63. Bradburn, S. How to Create a QQ Plot in Excel. Available online: https://toptipbio.com/qq-plot-excel/ (accessed on 20 January 2025).
64. Sopade, P.A. Criteria for an Appropriate Sorption Model Based on Statistical Analysis. *Int. J. Food Prop.* **2001**, *4*, 405–418. https://doi.org/10.1081/JFP-100108642.